

concentration observed in individual stratospheric IDPs ($1.7 \times 10^{-5} \text{ cm}^3 \text{ STP g}^{-1}$, ref. 6), the most ^3He -rich GPC-3 sediment (1,138–1,143 cm) carries ~ 7 p.p.m. by weight of IDPs small enough to retain helium. The He-bearing fraction corresponds to $\sim 1\%$ of the total IDP flux¹⁷, so the total IDP component in this interval is ~ 700 p.p.m. Assuming a chondritic Ir concentration of 481 p.p.m. (ref. 18), this 700 p.p.m. of IDPs contributes just 0.3 p.p.b. of Ir to the bulk sediment. A concentration of 0.3 p.p.b. amounts to only $\sim 15\%$ of the total Ir observed in the interval (~ 2 p.p.b., ref. 4) and is within the uncertainty of the Ir measurements⁴. This calculation demonstrates that ^3He is much more sensitive to the influx of extraterrestrial dust than is Ir.

Interplanetary dust reaching the Earth's atmosphere is thought to derive from both asteroidal and cometary debris in the Zodiacal Cloud^{19,6}. Although it is likely that gravitational effects favour both greater capture¹⁹ and lower degrees of heating²⁰ and He outgassing⁶ of asteroidal particles, both sources are thought to contribute to the present-day helium flux⁶. The observed ^3He flux variations are most simply attributed to changes in the abundance of dust in the Zodiacal Cloud associated with asteroidal breakup events and the passage of comets through the inner Solar System. In addition, changes in the solar output of energetic ^3He ions implanted into IDPs may modulate the average ^3He concentration in the infalling dust.

One of the most dramatic features in the implied flux record occurs near the end of the Eocene epoch. Between 37.6 and 36.3 Myr the implied flux nearly triples, a rise which is essentially indistinguishable from a step-function given bioturbation effects in the core. Within the age uncertainty of samples, this rise is synchronous with the occurrence of several tektite horizons observed around the world²¹. This correlation provides strong evidence for multiple terrestrial impact events associated with dust-bearing objects, possibly a comet shower. Evidence has also been presented for an unusually high abundance of impact craters in the Quaternary²², another period in which the implied ^3He flux is high. Further study of well-dated Cenozoic sediments is required to determine the origin of the ^3He flux variations and to evaluate the relationship between the ^3He record and known terrestrial impact events²². In particular a more detailed record of the rise and fall rates of the ^3He flux, and their temporal relation to evidence for impacts, would be very useful.

It has previously been suggested that subduction of IDP-bearing deep-sea sediments may account for the ^3He emitted by volcanoes²³, but this has been disputed both because helium can diffuse from IDPs during subduction¹¹ and because the absolute abundance of extraterrestrial helium in sediment seems insufficient^{24,25}. Although the GPC-3 data demonstrate that high $^3\text{He}/^4\text{He}$ ratios persist in deep-sea sediments for many millions of years, the flux of ^3He is actually lower than previously assumed²³. The GPC-3 results demonstrate that, throughout the Cenozoic era, the flux of IDP ^3He has been insufficient to supply the current emission from the mantle²⁴ even if all of the helium were subducted, and provides no new support for the idea that extraterrestrial helium plays a role in mantle geochemistry. □

Received 15 March; accepted 9 June 1995.

- Merrill, C. *Ann. N.Y. Acad. Sci.* **119**, 351–367 (1964).
- Kyriov, A. Y., Mamyrin, B. A., Silin, Y. I. & Khabarin, L. V. *Geochim. Int.* **10**, 202–205 (1973).
- Ozima, M., Takayanagi, M., Zashu, S. & Amari, S. *Nature* **311**, 449–451 (1984).
- Kyte, F. T., Leinen, M., Heath, G. R. & Zhou, L. *Geochim. cosmochim. Acta* **57**, 1719–1740 (1993).
- Corliss, B. H. & Hollister, C. D. in *The Ocean Floor* (eds Scrutton, R. A. & Talwani, M.) 277–304 (Wiley, New York, 1982).
- Nier, A. O. & Schlutter, D. J. *Meteorites* **25**, 263–267 (1990).
- Andrews, J. N. *Chem. Geol.* **49**, 339–351 (1985).
- Kurz, M. D., Jenkins, W. J., Hart, S. R. & Clague, D. *Earth planet. Sci. Lett.* **66**, 388–399 (1983).
- Takayanagi, M. & Ozima, M. *J. geophys. Res.* **92**, 12531–12538 (1987).
- Amari, S. & Ozima, M. *Nature* **317**, 520–522 (1985).
- Hiyagon, H. *Science* **263**, 1257–1259 (1994).
- Podosek, F. A., Honda, M. & Ozima, M. *Geochim. cosmochim. Acta* **44**, 1875–1884 (1980).
- Fukamoto, H., Nagao, K. & Matsuda, J. I. *Geochim. cosmochim. Acta* **50**, 2245–2253 (1986).

- Prince, R. A., Heath, G. R. & Kominz, M. *Geol. Soc. Am. Bull.* **91**, 1789–1835 (1980).
- Tilles, D. *Science* **153**, 981–985 (1966).
- Nier, A. O., Schlutter, D. J. & Brownlee, D. E. *Geochim. cosmochim. Acta* **54**, 173–182 (1990).
- Love, S. G. & Brownlee, D. E. *Science* **262**, 550–553 (1993).
- Anders, E. & Grevesse, N. *Geochim. cosmochim. Acta* **53**, 197–214 (1989).
- Flynn, G. J. *Planet. Space Sci.* **42**, 1151–1161 (1994).
- Flynn, G. J. *Icarus* **77**, 287–310 (1989).
- Keller, G., D'Hondt, S. & Vaillier, T. *Science* **221**, 150–152 (1983).
- Hut, P. et al. *Nature* **329**, 119–127 (1987).
- Anderson, D. L. *Science* **261**, 170–174 (1993).
- Trull, T. in *Noble Gas Geochemistry and Cosmochemistry* (ed. Matsuda, J.) 77–88 (Terrapub, Tokyo, 1994).
- Stuart, F. M. *Earth planet. Sci. Lett.* **122**, 245–247 (1994).

ACKNOWLEDGEMENTS. I thank F. Kyte, K. Turekian and B. J. Pegrarn for helpful comments and for supplying samples, and G. J. Flynn for a helpful review. This work was supported by the Ocean Sciences Division of the US National Science Foundation.

Unusual twentieth-century summer warmth in a 1,000-year temperature record from Siberia

Keith R. Briffa*, Phillip D. Jones*, Fritz H. Schweingruber†, Stepan G. Shiyatov‡ & Edward R. Cook§

* Climatic Research Unit, School of Environmental Sciences, University of East Anglia, Norwich NR4 7TJ, UK

† Swiss Federal Institute of Forest, Snow and Landscape Research, Zürcherstrasse 111, CH-8903 Birmensdorf, Switzerland

‡ Institute of Plant and Animal Ecology, Ural Branch of the Russian Academy of Sciences, 8 Marta Street, Ekaterinburg 620219, Russia

§ Tree-Ring Laboratory, Lamont-Doherty Earth Observatory, Columbia University, Palisades, New York 10964, USA

In the current debate on the magnitude of modern-day climate change, there is a growing appreciation of the importance of long, high-resolution proxies of past climate^{1–3}. Such records provide an indication of natural (pre-anthropogenic) climate variability, either singly at specific geographical locations or in combination on continental and perhaps even hemispheric scales⁴. There are, however, relatively few records that are well dated, of high resolution and of verifiable fidelity in terms of climate response, and conspicuously few that extend over a thousand years or more⁵. Here we report a tree-ring-based reconstruction of mean summer temperatures over the northern Urals since AD 914. This record shows that the mean temperature of the twentieth century (1901–90) is higher than during any similar period since AD 914.

Ring-width measurements from living and subfossil siberian larch (*Larix sibirica*) trees have previously been used to produce a continuous series representing interannual growth variability in a region centred on about 66° 50' N, 65° 15' E on the eastern side of the northern Urals, near Salekhard⁶. This mean ring-width chronology, running from AD 961 to AD 1969, formed the basis of a high-summer (June–July) season temperature reconstruction⁷. However, this reconstruction is of limited value in understanding 100-year timescale fluctuations, because of the way individual tree measurements were detrended to remove age-related sample bias in the mean chronology^{8,9} (a process known as 'standardization' in dendroclimatology^{9,10}). We have now resampled these trees, and analysed both living and subfossil material using wood densitometry to yield both ring-width and maximum-latewood-density time series¹¹ spanning the years from AD 914 to AD 1990. The density data were standardized so as to preserve variance at both short (internannual-to-decadal) and long (>100 years) timescales¹². The ring-width data were standardized using flexible smoothing splines, producing

TABLE 1 Relationships between tree growth and regional temperatures in the northern Urals

(a) Tree-growth temperature correlations																		
	Previous year				Year of tree growth												A1	A2
	S	O	N	D	J	F	M	A	M	J	J	A	S	O				
Density																		
1882–1935	0.08	0.01	0.17	0.02	0.11	0.07	0.05	0.15	0.44†	0.68†	0.59†	0.27*	0.32*	0.02	0.15	0.20		
1936–1990	-0.14	0.23	0.01	0.08	0.12	0.37†	-0.04	0.17	0.35*	0.64†	0.67†	0.39†	0.36†	-0.07	0.15	0.27*		
Ring width																		
1882–1935	0.24	0.07	0.11	0.29*	0.22	-0.14	-0.06	0.08	0.02	0.43†	0.55†	-0.10	0.19	0.14	0.29*	0.40†		
1936–1990	-0.03	0.25	0.11	-0.10	0.13	0.35	-0.10	-0.07	0.18	0.38†	0.49†	0.17	0.09	0.03	0.45†	0.26		
(b) May–September mean temperature regressions																		
Calibration period					1882–1935			1936–1990			1882–1990							
Verification period					1936–1990			1882–1935			—							
Calibration																		
Variance explained					0.70			0.66			0.68							
Verification																		
Variance explained					0.65			0.69										
Reduction of error					0.67			0.70										
Coefficient of efficiency					0.65			0.68										
First difference sign																		
Correct					46			44			—							
Incorrect					8			9			—							
Product mean <i>t</i>					5.4			3.9			—							
Regression weights																		
Max. density year <i>t</i>					1.10			1.10			1.11							
year <i>t</i> + 1					-0.11			-0.14			-0.14							
Ring width year <i>t</i>					-0.48			-0.56			-0.54							
year <i>t</i> + 1					0.20			0.34			0.27							

The density chronology was constructed by averaging measured values for all individual trees expressed as anomalies from a common empirically defined linear expression of declining density as a function of age. This straight-line reference was calculated as a least-squares fit to the observed average densities of all samples after aligning them with respect to their cambial age, regardless of their calendrical year of growth. The resulting indices, subsequently averaged across correct calendrical years, provide a chronology in which long-timescale variability is preserved and sample-age bias is largely eliminated¹². Separate standardizing equations were calculated for the modern and subfossil density data to explore the possibility of a systematic difference in the density/age relationship that might arise due to a slight elevational difference in these data sources (the subfossil samples being up to 80 m higher than the living trees). Such a difference might introduce a bias between the early and recent sections of the chronology. The similarity of the density/age equations derived from the separate subfossil (914–1744) and modern (1631–1990) samples argue against any long-term sample-related bias in the density chronology, although this does not preclude the possibility that changes in the average altitude of the samples through time might introduce some shorter-timescale bias where the replication is relatively low²⁸. The width chronology is the average of series for each tree after low-frequency variance, associated with a smoothing spline fit to the original measurements, has been removed. The frequency responses of the splines are tailored to the length of each series so that most of the variance on timescales longer than two-thirds the series length is removed. This produces a final ring-width chronology with low error variance, but with a spectrum that is truncated at low frequencies (that is, periods >50–100 years)²⁹. Individual monthly mean temperature correlations are shown with each of the maximum-latewood-density and ring-width chronologies. Also shown are the results of multiple regressions in which both the density and ring-width chronologies are used as predictors of mean May–September temperature. The results of verification tests^{10,30} are all highly statistically significant. A1 and A2 are the 1-year and 2-year lag autocorrelation coefficients.

* Significant at the 5% level.

† Significant at the 1% level or better.

a chronology characterized by variance on shorter timescales (generally below 100 years⁹) (see Table 1).

These chronologies were then used in a number of regression experiments designed to exploit the well-known dependence of tree growth on summer temperature variability at high latitudes^{13–16}. This is demonstrated in Table 1, which shows the density and ring-width chronologies correlated with monthly mean temperatures averaged within a region between 62.5° and 67.5° N, and 65° to 75° E¹⁷. All significant correlations are positive, indicating enhanced width and density associated with warmer temperatures. Correlations with ring width are greatest in June and July. Density correlations are stronger and manifest over a longer (May–September) season. The responses are also consistent in different periods. Mean May–September temperatures are very highly correlated ($r=0.95$ over 1881 to 1990) with cumulative growing degree days (>5 °C) in this region¹⁸. Regression results in which mean May–September temperatures are estimated as a function of density and width data in both the concurrent and following years (that is, *t* and *t* + 1 respectively), exhibit extremely strong predictive power (Table 1).

The explained variance over the calibration period (that is, 66–70%) and most importantly the levels explained in independent verification of the calculated regression equations (65–69%), and also the general levels of statistical significance associated with a number of stringent tests of model performance (see Table 1), all rank among the highest reported in the tree-ring literature. Regression based on the density predictors alone also explains a high degree of temperature variance (~60%) but consistently

less than that achieved using density and ring widths in combination.

The series (>1,000 years) of reconstructed summer temperatures for the northern Urals shows extended periods of either relatively cool or relatively warm summers persisting over 100–200 years (Fig. 1). Superimposed on this is large variability on annual and decadal timescales (Table 2). Despite relatively cool summers in the late 1960s and 1970s, the mean summer temperature of the twentieth century (1901–90) appears to be the warmest of any 90-year period during the last ten centuries (0.13 °C warmer than the next warmest period, 1202–91). Most of the sixteenth and seventeenth centuries were notably cool, particularly the 1530s and 40s, the 1580s and 90s, and the 1620s, 30s and 40s. The pronounced coolness of the late sixteenth and seventeenth centuries and the warmth of the twentieth century is shown in other, though shorter, high-latitude summer-responsive proxies¹⁹ and in an average of data from 16 selected sites in the Northern Hemisphere⁴ (Fig. 2a). However, the coldest bidecadal mean in the northern Urals data, 1531–50, indicates an earlier onset of the cold period seen in the mean 'hemisphere' data and in a similar millennial-length temperature reconstruction for northern Fennoscandia based on tree-ring data from Torneträsk, northwest Sweden, that were also processed so as to preserve long-timescale climate variability¹².

Although summers were predominantly warm in northern Fennoscandia in the eleventh and twelfth centuries, they were clearly cool in the northern Urals (Fig. 2b). This is further support for the sparse body of high-quality palaeoclimate evidence

now challenging the still prevalent, over-simplified concept of a globally synchronous, multi-century Mediaeval Warm Period^{5,20}. But after the coolness of the late sixteenth century, both the northern Urals and the northern Fennoscandian temperature curves show overall warming. Linear trends calculated over 1600–1980 show a 0.67 °C warming in northern Fennoscandia, but 1.14 °C over the northern Urals. The two series also display qualitatively similar century-scale trends, warming to the mid-eighteenth century, slight cooling to the end of the nineteenth century, followed by an abrupt rise and sustained warmth during the twentieth century. The recent warmth in Fennoscandia is not significant in a 1,000-year context¹². The recent warmth in the Urals data is much larger (compare Table 2) but because of the century-timescale variability in the reconstruction, assessing its statistical significance is not straightforward. A comparison of the mean values for the pre- and post-1900 periods, using a *t*-test which takes account of lag-1 serial correlation²¹ in the sample data, indicates that the likelihood of the unusual warmth of the twentieth century arising by chance is less than 1 in 1,000. However, an empirically derived probability distribution based on multiple artificial series with the same persistence structure as the reconstruction (that is, AR3 rather than AR1) suggests a probability near 1 in 100. We also compared (using a simple *t*-test) the 1901–90 mean with that of the next warmest 90-year period (1202–91, compare Table 2). This stringent test indicates that the two periods are significantly different with a probability of 1 in 10. So although the twentieth century was certainly unusually warm in the northern Urals, determining how unusual it was, in the context of the long record, is equivocal.

These results and the above discussion may be relevant to general circulation model (GCM) studies of both 'natural' and anthropogenically perturbed climates. Recent coupled ocean–

atmosphere GCM experiments with anthropogenic forcing indicate that maximum warming is likely in high-latitude and continental regions^{22,23}. There is, of course, uncertainty in defining this expected anthropogenic pattern. At present, this is best viewed as the spatial temperature response of coupled ocean–atmosphere GCMs forced with gradually changing atmospheric compositions²⁴. Attempts to detect this response pattern in observational temperature data must take account of natural variability of climate on long (>50–100 years) timescales. Also, simulated variability from long GCM control runs must be checked against long palaeoclimate series such as the one we report here.

Ocean–atmosphere GCMs also suggest that areas bordering the North Atlantic will experience reduced warming and even localized cooling near regions of deep-water formation^{22,23}. A recent 600-year simulation of climate variability under present-day boundary conditions has revealed significant quasi-periodicity in annual temperatures centred on the northwest Atlantic with characteristic timescales of between 40 and 60 years (ref. 25). Similar variability, explicable in terms of oceanic thermohaline forcing, has been observed in a number of different regional observational records and has the potential to obscure anthropogenic warming in the region of the North Atlantic^{26,27}. The northern Fennoscandian summer temperatures show

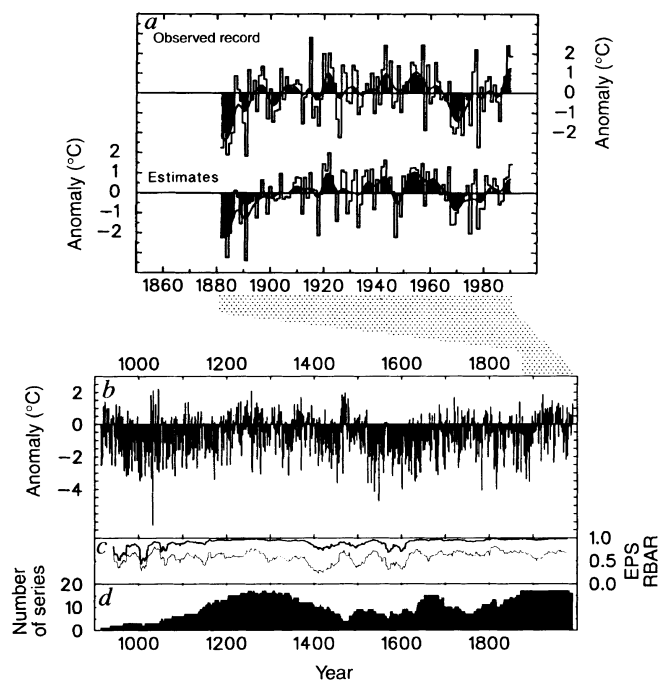


FIG. 1 a, Observed and estimated mean summer (May–September) temperatures over the northern Urals shown as anomalies (°C) from the 1951–70 mean. The smoothed line shows decadal-filtered values. b, The extended reconstruction (914–1990) expressed as anomalies from the same base. c, A measure of the strength of common growth 'signal' within the density chronology, the mean interseries correlation³¹ (RBAR; thin line) calculated between all samples over a moving 30-year window. The Expressed Population Signal (EPS; thick line) which is a function of RBAR and the series replication shown in d, indicates chronology reliability. Values >0.85 are generally considered satisfactory³¹.

TABLE 2 Extreme summer temperatures

(a) Individual summers

Warmest		Coldest	
Year	Anomaly (°C)	Year	Anomaly (°C)
1045	2.21	1032	-6.20
1033	2.11	1548	-4.73
1257	2.08	1538	-4.15
1471	1.96	1783	-4.08
1922	1.85	1816	-4.03
1464	1.84	1601	-4.01
1028	1.81	1531	-3.63
1468	1.70	1453	-3.62
1370	1.68	1523	-3.62
1720	1.65	1891	-3.55

(b) 20-year-mean periods

Warmest			Coldest		
Years	Anomaly	Standard error	Years	Anomaly	Standard error
1461–1480	0.45	0.27	1531–1550	-1.97	0.27
1948–1967	0.40	0.16	1623–1642	-1.85	0.26
1238–1257	0.34	0.17	998–1017	-1.75	0.24
1919–1938	0.24	0.23	1580–1599	-1.61	0.17
1355–1374	0.09	0.23	966–985	-1.44	0.29

(c) 50-year-mean periods

Warmest			Coldest		
Years	Anomaly	Standard error	Years	Anomaly	Standard error
1919–1968	0.23	0.14	1595–1644	-1.64	0.15
1208–1257	0.03	0.12	1522–1571	-1.55	0.15
1353–1402	-0.04	0.12	966–1015	-1.39	0.17
1460–1509	-0.13	0.14	1410–1459	-1.10	0.12
1261–1310	-0.18	0.13	1808–1857	-0.96	0.15

(d) 90-year-mean periods

Warmest			Coldest		
Years	Anomaly	Standard error	Years	Anomaly	Standard error
1901–1990	0.03	0.10	1522–1611	-1.52	0.10
1202–1291	-0.10	0.11	961–1050	-1.20	0.15
1301–1390	-0.28	0.10	1612–1701	-1.12	0.11

Extreme individual summer temperature estimates along with the extreme mean values from among all 20-year, 50-year and 90-year periods. Temperatures are shown as anomalies with respect to the 1951–70 period. Only values for non-overlapping periods are shown. Of the extreme individual summers, nine are reconstructed as cooler, and four warmer, than the reconstructed extremes (1891 and 1922) during the calibration period. Compared with the instrumental extremes (1891 and 1915), 15 summers are reconstructed as cooler but none warmer.

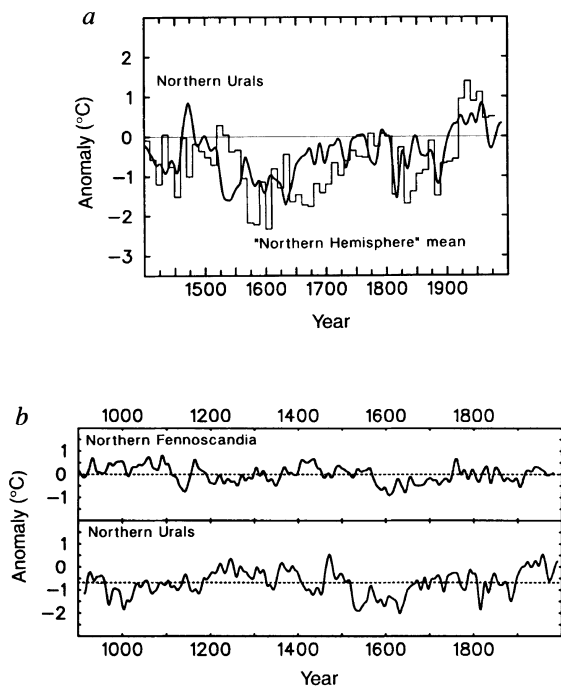


FIG. 2 *a*, The histogram shows 'mean Northern Hemisphere' summer temperatures⁴ constructed as standardized decadal averages of 16 proxy series, compared with northern Urals temperatures smoothed to emphasise decadal variability. Both series are expressed as anomalies from the 1860–1959 mean. The data from ref. 4 have been adjusted to give a standard deviation of one over the same period. *b*, Summer temperatures in northern Fennoscandia¹² and the northern Urals smoothed with a 25-year low-pass filter. The vertical axes are anomalies from the respective means for 1951–70. The dotted lines show the means for 901–1981 (northern Fennoscandia) and 914–1990 (northern Urals).

marked multi-decadal variance at periods near 33 years and over a range from 60 to 70 years (as well as longer periods) which may be associated with north Atlantic oceanic forcing^{12,26}.

Prolonged twentieth-century summer warmth over the Urals, and the slower rate of warming in recent centuries in northern Fennoscandia, are therefore at least consistent with the pattern of anthropogenically induced warming predicted by the models. Although the relative warmth through much of the thirteenth and fourteenth centuries means that statistical significance of the twentieth-century Urals warmth is equivocal, our results indicate that in this region no other period of this length has been warmer, at least during the past 1,000 years. A very limited number of high-resolution records indicate unprecedented recent warmth in other high-latitude regions, but this warmth is either observed over a shorter recent period or within a shorter overall timeframe. □

Received 6 December 1994; accepted 19 June 1995.

1. Eddy, J. A. Global IGBP Change Report No. 19 (International Geosphere–Biosphere Programme, Stockholm, 1992).
2. Bradley, R. S. (ed.) *Global Changes of the Past* (University Corporation for Atmospheric Res./Office of Interdisciplinary Earth Studies, Boulder, 1991).
3. Bradley, R. S. & Jones, P. D. (eds) *Climate Since A.D. 1500* (Routledge, London, 1992).
4. Bradley, R. S. & Jones, P. D. *The Holocene* **3**, 367–376 (1993).
5. Hughes, M. K. & Diaz, H. F. *Clim. Change* **26**, 109–142 (1994).
6. Shiyatov, S. G. *Dendrochronology in the Upper Tree Line in the Urals* (Nauka, Moscow, 1986) (in Russian).
7. Graybill, D. A. & Shiyatov, S. G. in *Climate Since A.D. 1500* (eds Bradley, R. S. & Jones, P. D.) 393–414 (Routledge, London, 1992).
8. Shiyatov, S. G. & Mazepa, V. S. in *Methods of Dendrochronology* Vol. 1 (eds Kairiukstis, L. A., Bednarz, Z. & Feliksik, E.) 87–96 (IASA/Polish Acad. Sci.—Systems Res. Inst., Warsaw, 1987).
9. Cook, E. R., Briffa, K. R., Shiyatov, S. G. & Mazepa, V. S. in *Methods of Dendrochronology* (eds Cook, E. R. & Kairiukstis, L. A.) 104–123 (Kluwer/IASA, Dordrecht, 1990).
10. Fritts, H. C. *Tree Rings and Climate* (Academic, London, 1976).
11. Schweingruber, F. H. *Tree Rings: Basics and Applications of Dendrochronology* (Reidel, Dordrecht, 1988).

12. Briffa, K. R. et al. *Clim. Dyn.* **7**, 111–119 (1992).
13. Jacoby, G. C. & Cook, E. R. *Arct. Alp. Res.* **13**, 409–418 (1981).
14. Briffa, K. R., Jones, P. D., Pilcher, J. R. & Hughes, M. K. *Arct. Alp. Res.* **20**, 385–394 (1988).
15. Briffa, K. R. et al. *Nature* **346**, 434–439 (1990).
16. Schweingruber, F. H., Briffa, K. R. & Nogler, P. *Int. J. Biomet.* **37**, 151–169 (1993).
17. Jones, P. D. et al. *J. Clim. appl. Met.* **25**, 161–179 (1986).
18. Jones, P. D. & Briffa, K. R. *Int. J. Climatol.* (in the press).
19. D'Arrigo, R. D. & Jacoby, G. C. Jr in *Climate Since A.D. 1500* (eds Bradley, R. S. & Jones, P. D.) 296–311 (Routledge, London, 1992).
20. Folland, C. K., Karl, T. R. & Vinnikov, K. Ya. in *Climate Change: the IPCC Assessment* (eds Houghton, J. T., Jenkins, G. J. & Ephraums, J. J.) 195–238 (WMO/UNEP, Cambridge Univ. Press, 1990).
21. Zwiers, F. W. & von Storch, H. *J. Clim.* **8**, 336–351 (1995).
22. Cubasch, U. et al. *Clim. Dyn.* **8**, 55–69 (1992).
23. Gates, W. L., Mitchell, J. F. B., Boer, G. J., Cubasch, U. & Meleshko, V. P. in *Climate Change 1992: The Supplementary Report to the IPCC Scientific Assessment* (eds Houghton, J. T., Callander, B. A. & Varney, S. K.) 97–134 (WMO/UNEP, Cambridge Univ. Press, 1992).
24. Santer, B. D. et al. *Clim. Dyn.* (in the press).
25. Delworth, T., Manabe, S. & Stouffer, R. J. *J. Clim.* **6**, 1993–2011 (1993).
26. Stocker, T. F. *Nature* **367**, 221–222 (1994).
27. Schlesinger, M. E. & Ramankutty, N. *Nature* **367**, 723–726 (1994).
28. Briffa, K. R., Jones, P. D., Schweingruber, F. H., Karlén, W. & Shiyatov, S. G. in *Climate Fluctuations and Forcing Mechanisms of the Last 2,000 Years* (eds Jones, P. D., Bradley, R. S. & Jouzel, J.) (Springer, Berlin, in the press).
29. Cook, E. R. & Briffa, K. R. in *Methods of Dendrochronology* (eds Cook, E. R. & Kairiukstis, L. A.) 153–162 (Kluwer/IASA, Dordrecht, 1990).
30. Cook, E. R., Briffa, K. R. & Jones, P. D. *Int. J. Climatol.* **14**, 379–402 (1994).
31. Wigley, T. M. L., Briffa, K. R. & Jones, P. D. *J. Clim. appl. Met.* **23**, 201–213 (1984).

ACKNOWLEDGEMENTS. We thank E. Schär for densitometric analysis, and M. K. Hughes, T. M. L. Wigley and F. W. Zwiers for comments that helped in rewriting an earlier version of the manuscript. This work was supported by the University of East Anglia Innovation Fund and the EC Environment Research Programme (K.R.B.), the Swiss National Science Foundation (F.H.S.) and the US Dept of Energy (P.D.J.).

Longevity of sub-continental mantle lithosphere from osmium isotope systematics in orogenic peridotite massifs

L. Relsberg* & J.-P. Lorand†

* Centre de Recherches Pérographiques et Géo-chimiques (CRPG/CNRS), BP 20, 54501 Vandoeuvre-lès-Nancy, France

† Laboratoire de Mineralogie, URA CNRS 716, 61 Rue Buffon, Museum National d'Histoire Naturelle, 75005 Paris, France

ATTEMPTS to understand the formation and evolution of the sub-continental lithospheric mantle (SCLM) have been hampered by the absence of reliable time constraints, reflecting a lack of appropriate isotopic dating techniques. The most commonly used methods, involving strontium, neodymium and lead isotopes, yield ambiguous results in mantle rocks, and show no relationship with magmatic processes, as the low concentrations of these elements make them susceptible to later metasomatic disturbance. Osmium, by contrast, is much more abundant in the mantle than in the crust¹, so that peridotite Os isotope ratios are largely immune to recent metasomatic imprints. This provides a way to date the magmatic processes that determine mantle major-element compositions². We present here two examples of striking correlations between ¹⁸⁷Os/¹⁸⁸Os and Al₂O₃ concentration in orogenic peridotites, and argue that these can be used to date the differentiation of the SCLM. The old ages obtained agree with associated lower-crustal Nd model ages^{3–5}, and indicate that—in these post-Archaeon terrains as well as in Archaean cratons^{2,6,7}—SCLM can remain isolated from the convecting mantle for more than a billion years.

Orogenic peridotite massifs are slices of upper mantle that have been tectonically emplaced into the crust. They contain small proportions of mafic veins and layers, but are dominated by peridotites, which range in composition from clinopyroxene-rich lherzolites to clinopyroxene-poor harzburgites. The two such massifs discussed here are the Ronda Ultramafic Complex of southern Spain and the eastern Pyrenean peridotites. Ronda, a large contiguous ultramafic massif in the Betic–Rif Cordillera,